The Journal of Experimental Biology 210, 522-532
Published by The Company of Biologists 2007
doi:10.1242/jeb.02679

The interaction of CO_2 concentration and spatial location on O_2 flux and mass transport in the freshwater macrophytes *Vallisneria spiralis* and *V. americana*

Gregory N. Nishihara[1] and Josef D. Ackerman[1,2,*]

[1]*Department of Integrative Biology and* [2]*Faculty of Environmental Sciences, University of Guelph, Guelph, Ontario, N1G 2W1, Canada*

*Author for correspondence (e-mail: ackerman@uoguelph.ca)

Accepted 5 December 2006

Summary

The biology of aquatic organisms determines the maximum rates of physiological processes, but the mass transport of nutrients determines the nominal rates at which these processes occur. Maximum O_2 flux (P_{max}) at 17.1 mmol m^{-3} CO_2 was higher for the leaves of the freshwater macrophyte *Vallisneria spiralis* [P_{max}=0.013±0.001 mmol m^{-2} s^{-1} (g_{chla+b} m^{-2})$^{-1}$ (mean ± s.e.m.)] than for the closely related species, *Vallisneria americana* [P_{max}=0.008±0.001 mmol m^{-2} s^{-1} (g_{chla+b} m^{-2})$^{-1}$]. The O_2 flux saturated at freestream velocities >4.5±1.2 cm s^{-1} and was spatially invariant for both species. However, a tenfold decrease in CO_2 concentration to 1.71 mmol m^{-3} changed the nature of the relationship between O_2 flux and spatial location along the leaf surface, and reduced the O_2 flux of *V. spiralis* to values similar to *V. americana*. The O_2 flux [P_{max}=0.007±0.001 mmol m^{-2} s^{-1} (g_{chla+b} m^{-2})$^{-1}$] saturated at the upstream location (i.e. 1 cm from the leading edge of the leaf) but was found to increase linearly with freestream velocity [slope=0.057±0.011 mmol m^{-2} s^{-1} (g_{chla+b} m^{-2})$^{-1}$ (m s^{-1})$^{-1}$] at the downstream location (i.e. 7 cm from the leading edge) at freestream velocities >1.8±0.9 cm s^{-1}. Conversely, mass transfer rates did not vary with CO_2 concentration, and were characteristic of a laminar concentration boundary layer at the upstream location and a turbulent concentration boundary layer at the downstream location. Rates of mass transfer measured directly from O_2 profiles were not predicted by theoretical values based on hydrodynamic measurements. Moreover, the concentration boundary layer thickness (δ_{CBL}) values measured directly from O_2 profiles were 48±2% and 21±1% of the predicted theoretical δ_{CBL} values at the upstream and downstream locations, respectively. It is evident that physiological processes involving mass transport are coupled and vary in space. Mass transport investigations of biological systems based solely on hydrodynamic measurements need to be interpreted with caution.

Key words: hydrodynamics, morphology, photosynthesis, kinetic limitation, mass transfer limitation, DIC, carbon uptake, concentration boundary layer, momentum boundary layer.

Introduction

The ecophysiological processes of aquatic organisms are diverse, and the form and rate of these processes vary within and among species (Phillips and Hurd, 2004; Nishihara et al., 2005; Badgley et al., 2006). In the case of aquatic macrophytes, variations in processes such as nutrient uptake and photosynthesis are influenced by abiotic and biotic conditions (e.g. nutrient history, nutrient concentration, water flow, temperature and light) (Hurd et al., 1996; Nishihara et al., 2005; Badgley et al., 2006). The kinetics of these mass transfer and uptake processes can be linear or nonlinear and can differ among nutrients and species. For example, in the red alga *Laurencia brongniartii*, the uptake kinetics were linear for nitrate and nonlinear for ammonium (Nishihara et al., 2005), whereas nonlinear kinetics were observed for both nutrients in the brown alga *Scytothamnus australis* (Phillips and Hurd, 2004). Indeed, physiology ultimately determines the rate of such processes; however, the transport of nutrients to the surface of aquatic macrophytes governs whether the process is kinetically or mass transfer limited (Sanford and Crawford, 2000; Nishihara and Ackerman, 2006).

Dissolved inorganic carbon (DIC) is available to aquatic macrophytes in the form of CO_2 and HCO_3^- (Madsen and Sand-Jensen, 1991). Whereas HCO_3^- is the primary form of DIC available in marine environments due to relatively high pH, the dominant form of DIC in freshwater varies with ambient pH. However, in cases where alkalinities are low, freshwater macrophytes have greater access to dissolved CO_2. Increases in CO_2 concentrations are, therefore, thought to benefit freshwater and marine macrophytes capable of HCO_3^- uptake that have a higher affinity (i.e. sensitivity) for CO_2 (Madsen and Sand-Jensen, 1991; Invers et al., 2001). In general, DIC uptake

(i.e. photosynthesis) can be described by a rectangular hyperbola, where for low DIC, photosynthesis rates are directly proportional to the DIC concentration, and for large DIC, photosynthesis rates are saturated (Maberly and Madsen, 1998; Invers et al., 2001; Nishihara and Ackerman, 2006). The delivery of DIC to supply photosynthesis occurs through diffusive and advective transport, and differences in rates occur as a result of the different concentrations and diffusivities of CO_2 and HCO_3^-. Indeed, in calm water, diffusive transport can serve as the primary mechanism by which DIC is transported to a macrophyte, whereas in flowing water advective transport becomes the dominant mechanism of mass transport. Increased DIC mass transfer rates resulting from advection can also supply proportionately more DIC in the form of CO_2 (Nishihara and Ackerman, 2006). Therefore, the ecophysiology of aquatic macrophytes is influenced by the mass transport of nutrients, and in conditions where water velocities and ambient concentrations are low, productivity can be limited by mass transport (Stevens and Hurd, 1997; Cornelisen and Thomas, 2006; Nishihara and Ackerman, 2006).

Mass transfer rates are a function of the freestream velocity (U), the molecular diffusivities (D) of DIC, the concentration gradient ($\Delta C=C_S–C_B$) between the bulk water (C_B) and the surface concentrations (C_S), and the geometry of the macrophyte. An increase in U or ΔC will increase mass transfer rates and thus provide more DIC, leading to higher rates of photosynthesis (Nishihara and Ackerman, 2006). Mass transfer rates may vary with location, as in the case of a flat plate oriented parallel to the flow, where mass transfer rates decrease monotonically with increasing downstream direction (Schlichting and Gersten, 2000). Whether the mass transfer rates of nutrients vary spatially over the surface of a macrophyte, and thus influence physiological processes, remains to be determined.

The freshwater angiosperms, *Vallisneria spiralis* L. and *Vallisneria americana* Michx., are found throughout Europe and North America, respectively, and occupy similar niches in their respective environments (Sculthorpe, 1967). Both species can assimilate HCO_3^- (Prins et al., 1980; Madsen and Sand-Jensen, 1991) and can be found in waters high in alkalinity (i.e. 100–1400 mmol m^{-3} HCO_3^-) (Pip, 1984). More importantly, a key morphological trait that differentiates the two is the spiral twist found in *V. spiralis* (Fig. 1A), unlike the relatively flat leaves of *V. americana* (Fig. 1B). Little is known about the function of the twist; however, morphological features, which present a more complex geometry than that of a flat surface, have been found to enhance mass transport and physiological processes in other aquatic organisms (Hurd et al., 1996; Falter et al., 2005). *V. spiralis* and *V. americana* provide an excellent opportunity to determine whether and how physiological processes are influenced by physical and environmental factors in two closely related species. The objective of this study is, therefore, to determine: (1) how the O_2 flux of *V. spiralis* and *V. americana* is influenced by CO_2 concentrations and velocity; (2) how O_2 flux and mass transfer rates vary with respect to spatial location; and (3) how a flat and twisted leaf morphology affects O_2 flux and mass transport.

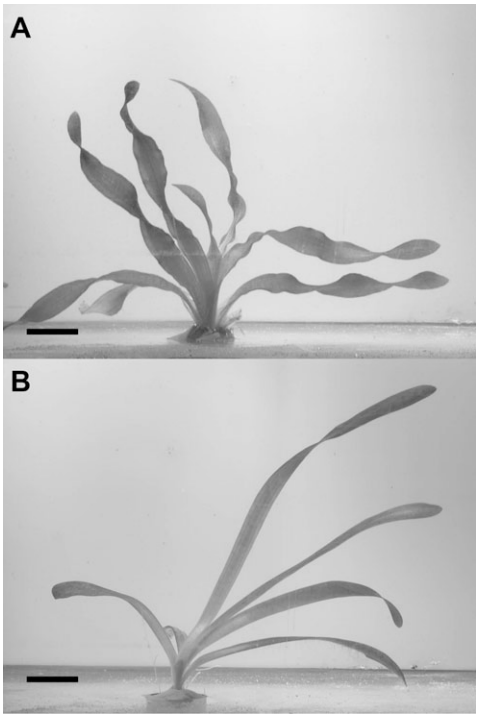

Fig. 1. *Vallisneria spiralis* (A) and *Vallisneria americana* (B) in a flow chamber at a freestream velocity of 6 cm s^{-1}. The flow is from left to right; scale bar, 2 cm.

Materials and methods

Aquatic macrophytes

Vallisneria spiralis L. and *V. americana* Michx. (obtained from Boreal Laboratories) were grown in 20 l aquaria, using nutrient enriched wellwater at 25°C and a soil substrate (Nishihara and Ackerman, 2006). The photosynthetically active radiation (PAR) level was maintained at 7.3 μmol photon m^{-2} s^{-1} (16 h:8 h L:D), as measured in the center of the aquaria with a 4π sensor (QSL2101, Biospherical Instruments, San Diego, CA, USA), to discourage the growth of microalgae and other potential fouling organisms.

Experimental setup

The experimental setup is described in detail elsewhere (Nishihara and Ackerman, 2006; Nishihara and Ackerman, 2007). Briefly, a 10 cm×10 cm×100 cm long (water depth: 5–8 cm) flow chamber, with flow straighteners in the first 12 cm, was operated at freestream velocities of 0.5, 0.8, 1.1, 1.8, 2.1, 3.3, 4.1 and 6.6 cm s^{-1}. Velocity profiles in the empty flume were determined using digital particle image velocimetry (PIV) at the location of the leading edge of the leaf (56 cm downstream of the flow straighteners), and were uniform in shape, especially at the height where the O_2 profiles were obtained above leaf surfaces (3 cm above the flume bottom) (Nishihara and Ackerman, 2006). The flow chamber water was maintained at 24°C, and aerated to maintain O_2 and CO_2 saturation, using a mixture of tapwater [pH=9.2±0.2 (mean ± s.e.m.)] and

deionized water having a final HCO_3^- concentration of 460 mmol m^{-3}. PAR (153 μmol photon m^{-2} s^{-1}) was provided by a slide projector with a quartz lamp (General Electric, Fairfield, CT, USA) adjusted with neutral density filters. The bulk O_2 concentration and O_2 profiles in the CBL were determined using OXN and OX25 oxygen microsensors (Unisense, Aarhus, Denmark), respectively. The O_2, pH and water temperature were recorded continuously by a computer.

V. spiralis and *V. americana* leaves were selected from the culture that were: (1) free of obvious epiphytes; (2) at least 8 cm long; (3) twisted only once in a 8 cm span in the case of *V. spiralis*; and (4) without undulations along the length and width of the leaf in the case of *V. americana*. The leaves were trimmed to size (8 cm in length), the cut ends were sealed with wax, and allowed to acclimate overnight in the flow chamber water. Leaf sections were glued (cyanoacrylate-based adhesive) to a wire stand, and placed in the working section of the flow chamber, perpendicular to the light source, and parallel to the flow. After each experiment, images of sections of the leaf approximately 1 cm^2 from the upstream and downstream locations (i.e. 1 cm and 7 cm from the leading edge of the leaf, respectively) were taken and the samples were frozen (–20°C) for later chlorophyll a+b analysis. $Chlorophyll_{a+b}$ content was determined as described (Nishihara and Ackerman, 2006). These two closely related species were chosen in part because their physiologies were assumed to be similar.

Measured variables

The effect of the experimental factors (i.e. species-leaf configuration, upstream *vs* downstream measurement location on the leaf surface, CO_2 concentration and velocity) on O_2 flux, mass transport and the thickness of the concentration boundary layer (δ_{CBL}) were investigated by profiling the O_2 concentration above the leaves (z=0–0.5 cm) of each leaf at x=1 and 7 cm downstream from the leading edge of the leaf (i.e. the upstream and downstream locations). The CO_2 concentration was adjusted to 1.71 mmol m^{-3} and 17.1 mmol m^{-3} by adding 50 mmol m^{-3} Tris buffer and appropriate amounts of HCl (i.e. to obtain a pH of 7.5 and 8.5, respectively) to the water in the flow chamber (Stumm and Morgan, 1996). During the course of the experiments pH and HCO_3^- concentrations remained stable, regardless of aeration, and no negative effects of the buffer on photosynthesis were observed. At least 5 min elapsed prior to determining the O_2 profiles for each species-leaf configuration, measurement location, and CO_2 concentration at all U and a randomized block design was used to minimize the effects of acclimation time. A total of nine *V. spiralis* and six *V. americana* leaves were analyzed at 1.71 mmol m^{-3} CO_2 and six *V. spiralis* and six *V. americana* leaves were analyzed at 17.1 mmol m^{-3} CO_2. Eight *V. americana* leaves were also reconfigured from a flat to twisted configuration by gently twisting the leaf to mimic *V. spiralis*, and maintaining the abaxial surface to the O_2 microsensor. In this case, experiments were conducted at 17.1 mmol m^{-3} CO_2 at the downstream location in the flat and twisted configurations.

Theory

The O_2 flux (J), mass transfer coefficient (k_c), and the concentration boundary layer thickness (δ_{CBL}) were determined by fitting a hyperbolic tangent model to the measured O_2 profiles (Nishihara and Ackerman, 2007):

$$\theta = \alpha \tanh\left(\frac{b}{a} z\right), \quad (1)$$

where $\theta=(C_S–C)/(C_S–C_B)$ is the dimensionless concentration, a is a parameter that describes the slope of the model at z=0, and b is a parameter that defines the invariant portion of the O_2 profile. By taking the first derivative of the model and evaluating the concentration gradient at the leaf surface (z=0), J can be determined from Fick's first law:

$$J = D \left.\frac{d\theta}{dz}\right|_{z=0}, \quad (2)$$

where D is the molecular diffusivity of O_2 in water (i.e. 2.4×10^{-9} m^2 s^{-1} at 24°C). J was normalized by the $chlorophyll_{a+b}$ (chl_{a+b}) concentration determined for each leaf position prior to the analyses, and this normalized O_2 flux is referred to as O_2 flux (J_{chla+b}) hereafter. Importantly, this normalization removes the possibility that tissue age may influence the O_2 flux, given that lower concentrations of chl_{a+b} have been noted in young and old tissue (Jana and Choudhuri, 1980).

To determine how the experimental factors influence O_2 flux, the relationship between O_2 flux (J_{chla+b}) and velocity were analyzed through linear and a nonlinear regression, using:

$$J_{chla+b} = \frac{J_{max}U}{V+U}, \quad (3)$$

where V is the half-saturation velocity and J_{max} is the maximum O_2 flux. A saturation velocity (V_{sat}) can be defined, where V_{sat}=9V is the value of U when J_{chla+b} is 90% of J_{max} (Nishihara and Ackerman, 2006).

The mass transfer of O_2 was analyzed by determining the local Sherwood number (Sh_x) for each mass transfer coefficient (k_c) determined from the O_2 profiles. k_c was calculated by dividing J by the O_2 concentration gradient (ΔC) between the leaf surface and bulk water. Sh_x, which is the ratio of the advective to diffusive flux that provides a measure of the relative importance of advection, was determined by:

$$Sh_x = \frac{k_c x}{D}. \quad (4)$$

A local Reynolds number (Re_x), which is the ratio of inertial to viscous forces in the boundary layer above the leaf, was determined to elucidate the effects of U and x on Sh_x, by:

$$Re_x = \frac{Ux}{\nu}, \quad (5)$$

where ν is the molecular diffusivity of momentum (0.922×10^{-6} m^2 s^{-1} at 24°C), recognizing that:

$$Sh_x = ARe_x^B Sc^C , \quad (6)$$

where A is a function of the flow properties, leaf geometry and orientation, and leaf physiology (Schuepp, 1993) and B and C are a function of the flow regime. When rates of physiological processes are slow compared to mass transfer rates (i.e. kinetic limitation) and the concentration boundary layer is laminar, A=0.464, B=0.5 and C=0.33, whereas when the concentration boundary layer is turbulent, A=0.030, B=0.8 and C=0.6 (Kays et al., 2005). *Sc* is the Schmidt number, which is the ratio of the momentum diffusivity to the molecular diffusivity. A linear regression of the double log plot of Sh_x/Sc^C *vs* Re_x provides estimates of parameters A and B. Parameter C was set to 0.33 for the analysis, since there was no *a priori* way of determining the regime of the boundary layer. Note that this in no way affects the estimates of B, which is the parameter of interest in this study, since Sc^C is constant at the experimental conditions investigated (*Sc*=384 for O_2 at 24°C).

For a laminar concentration boundary layer, δ_{CBL} was determined from the model fit to the measured O_2 profiles (Eqn 1) and is defined as the distance from the leaf surface where the O_2 concentration is 99% of the bulk concentration (Nishihara and Ackerman, 2007). The relationship between δ_{CBL} and U and x can be analyzed in a form similar to that of Eqn 6, by substituting Sh_x with $\delta_{CBL}x^{-1}Sc^{-0.33}$, recognizing that the δ_{CBL} can be expressed as:

$$\delta_{CBL} = 5xRe_x^{-0.5}Sc^{-0.33} . \quad (7)$$

In the case of a turbulent concentration boundary layer, a diffusive sublayer thickness (δ_{DSL}) can be defined, where diffusive transport becomes important (i.e. analogous to a laminar concentration boundary layer) (Dade, 1993),

$$\delta_{DSL} = \frac{10\nu}{u^*} Sc^{-0.33} . \quad (8)$$

In this case, the shear velocity (u^*) can be estimated from the relation $\tau=\rho u^{*2}$, where ρ is the density of water and τ is the boundary shear stress determined from the 1/7 power-law (White, 1999).

k_c, Sh_x and the δ_{DSL} can also be determined from hydrodynamic measurements of the momentum boundary layer (Nishihara and Ackerman, 2006). Vertical profiles of the momentum boundary layer at the upstream and downstream locations were obtained for *V. spiralis* and *V. americana* in the flat and twisted configurations using PIV. Shear velocities, which were determined by multiplying the von Karman constant (κ=0.41) by the slope of the velocity *vs* ln(*z*) in the logarithmic portion of the boundary layer (Ackerman and Hoover, 2001), were used to estimate k_c and the δ_{DSL} (Dade, 1993) where:

$$k_c = 0.1u^*Sc^{-0.67} , \quad (9)$$

and the δ_{DSL} is determined from Eqn 8. The Sh_x in a turbulent concentration boundary layer is determined by substituting k_c into Eqn 4.

Statistical analysis

Statistica 6.1 (Statsoft, Inc., Tulsa, OK, USA) and R (R Development Core Team, 2006) were used to analyze the data. Linear and nonlinear regressions were used as appropriate, and an *F*-test was used to determine whether these were significant, ANCOVA was used to determine whether differences in slopes of the linear regressions were significant, and Tukey's test was used to examine multiple comparisons. For regression analyses of Sh_x and δ_{CBL}, determined from O_2 profiles, log(Re_x) was the covariate and species-leaf configuration (i.e. *V. spiralis*, *V. americana* and *V. americana* in the twisted configuration), position and CO_2 concentration were the factors. In the case of PIV determined Sh_x and δ_{DSL}, log(Re_x) was the covariate and species-leaf configuration and measurement location were the factors. Significance was defined at P=0.05 and values are reported as mean ± s.e.m., except for the nonlinear regressions where s.e.m. is asymptotic.

Results

O_2 flux

The O_2 flux at the upstream and downstream locations of *V. spiralis* and both leaf configurations of *V. americana* increased monotonically with increasing velocity at 17.1 and 1.71 mmol m^{-3} CO_2 (Fig. 2). The O_2 flux was also similar to those previously determined for *V. americana* (dotted line in Fig. 2) (Nishihara and Ackerman, 2006) and is comparable to other studies involving aquatic macrophytes (Madsen and Sand-Jensen, 1991).

The relationship between the O_2 flux and velocity, determined at 17.1 mmol m^{-3} CO_2, can be described by a rectangular hyperbola for both species and measurement locations, where J_{max} is the maximum O_2 flux and V is the half-saturation velocity (Fig. 2A; Table 1). An *F*-test revealed that there was no significant difference ($F_{(30,34)}$=0.43, P=0.79) between a common V model (unique J_{max}) and the full model (unique V and J_{max} for each species and position), therefore the common V model (r^2=0.32, $F_{(6,34)}$=3.94, P=0.0064) was applied to describe O_2 flux at 17.1 mmol m^{-3} CO_2 (Fig. 2A and Table 1). Overall, O_2 flux was higher for *V. spiralis* compared to *V. americana*. J_{max} determined from the model was greatest for *V. spiralis* (P<0.05); however, there was no measurement location effect (P>0.05) within species. V_{sat} at 17.1 mmol CO_2 was 4.5±1.2 cm s^{-1}, which was similar to an earlier investigation of *V. americana* (V_{sat}=4±1 cm s^{-1} at 460 mmol m^{-3} DIC) (Nishihara and Ackerman, 2006).

In contrast, the relationship between the O_2 flux at 1.71 mmol m^{-3} CO_2 and U varied with location along the leaf, but not with species (Fig. 2B). O_2 profiles were difficult to determine at the higher velocities for *V. spiralis* and *V. americana* at this CO_2 concentration because the concentration gradient was too thin to profile. Specifically, eight downstream O_2 profiles were obtained at 4.1 and 6.6 cm s^{-1} for *V. spiralis*,

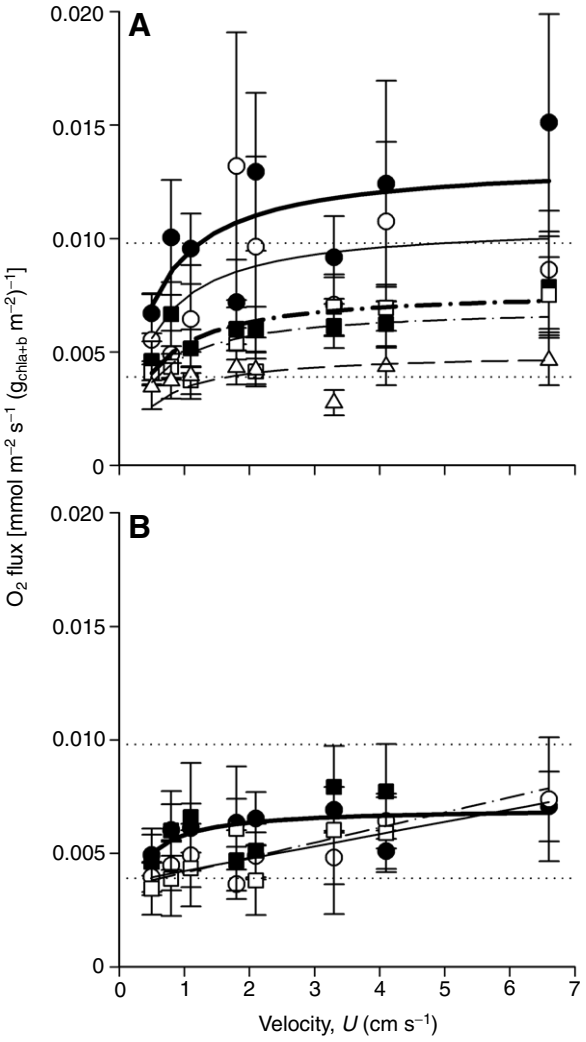

Fig. 2. O_2 flux determined from O_2 profiles at the upstream location (filled symbols) and downstream locations (open symbols) of *Vallisneria spiralis* (circles) and *Vallisneria americana* in a flat (squares) and twisted configuration (triangles) at (A) 17.1 mmol m^{-3} CO_2 and (B) 1.71 mmol m^{-3} CO_2. Solid lines are model fits for *V. spiralis*, dash-dotted lines are for *V. americana* in a flat configuration, and the broken lines are for *V. americana* in a twisted configuration. Thick lines fit the model data at the upstream location and the thin lines are fit to the downstream location. Note that for Fig. 1B, the models at the leading edge overlap. The two horizontal dotted lines indicate the range of O_2 fluxes determined from *V. americana* at ~0.171 mmol m^{-3} CO_2 (Nishihara and Ackerman, 2006). Values are means ± s.e.m. In A, N=6 for *V. spiralis*, N=6 for *V. americana* in the flat configuration and N=8 for *V. americana* in the twisted configuration. In B, N=9 for *V. spiralis* and N=6 for *V. americana* in the flat configuration.

compared to *V. americana* where five profiles were obtained at 3.3 and 4.1 cm s^{-1} and none at 6.6 cm s^{-1} at the upstream location; only four profiles at 4.1 cm s^{-1} and two profiles at 6.6 cm s^{-1} were obtained at the downstream location. Nevertheless, the O_2 flux at the upstream location was greater than the downstream location when $U<V_{sat}$=1.8±0.9 cm s^{-1} (Fig. 2B). The O_2 flux was nonlinear at the upstream location, and Eqn 3 was fit to the data. An F-test revealed that the most appropriate model for this location was a reduced form (common V and J_{max} in Eqn 3; r^2=0.26, $F_{(2,13)}$=2.94, P=0.026), since neither a full model nor a common V model was significant ($F_{(11,13)}$=0.26, P=0.79 and $F_{(11,12)}$=0.48, P=0.50, respectively) (Table 1). In contrast, at the downstream location, O_2 flux appeared to increase linearly with U, and a linear model was applied to the data. In this case, an ANCOVA revealed that the slopes for the two species were not significantly different ($F_{(1,11)}$=0.23, P=0.64) and species had no effect on O_2 flux ($F_{(1,12)}$=0.023, P=0.88), therefore a common linear model was applied to these data (r^2=0.67, $F_{(1,13)}$=29.61, P<0.0001) (Table 1).

Mass transfer

The Sh_x for the O_2 profiles increased with Re_x for all species-leaf configurations, CO_2 concentrations, and measurement locations (Fig. 3). Measurement location had a significant effect on the slope of the regressions ($F_{(2,58)}$=9.94, P=0.0002)

Table 1. *Parameters for the rectangular hyperbola and linear models describing the relationship between the chlorophyll$_{a+b}$-normalized O_2 flux and freestream velocity of the freshwater macrophytes, Vallisneria spiralis and Vallisneria americana, determined upstream or downstream from the leading edge of the leaf*

[CO_2] (mmol m^{-3})	Species	N	Location	Model	Chlorophyll$_{a+b}$-normalized O_2 flux [mmol m^{-2} s^{-1} (g_{chla+b} m^{-2})$^{-1}$]	
					P_{max} or Slope	V or Intercept
17.1	*V. spiralis*	6	US	Nonlinear	0.013±0.0010***	0.45±0.14**
17.1	*V. spiralis*	6	DS	Nonlinear	0.011±0.0009***	0.45±0.14**
17.1	*V. americana*	6	US	Nonlinear	0.008±0.0008***	0.45±0.14**
17.1	*V. americana*	6	DS	Nonlinear	0.007±0.0008***	0.45±0.14**
17.1	*V. americana* (twisted)	8	DS	Nonlinear	0.005±0.0008***	0.45±0.14**
1.71	Both	15	US	Nonlinear	0.007±0.0005***	0.20±0.10 (P=0.07)
1.71	Both	15	DS	Linear	0.057±0.0105***	0.36±0.03**

US, upstream, x=1 cm; DS, downstream, x=7 cm.
Values for P_{max} and V are means ± s.e.m. **P<0.01; ***P<0.001.

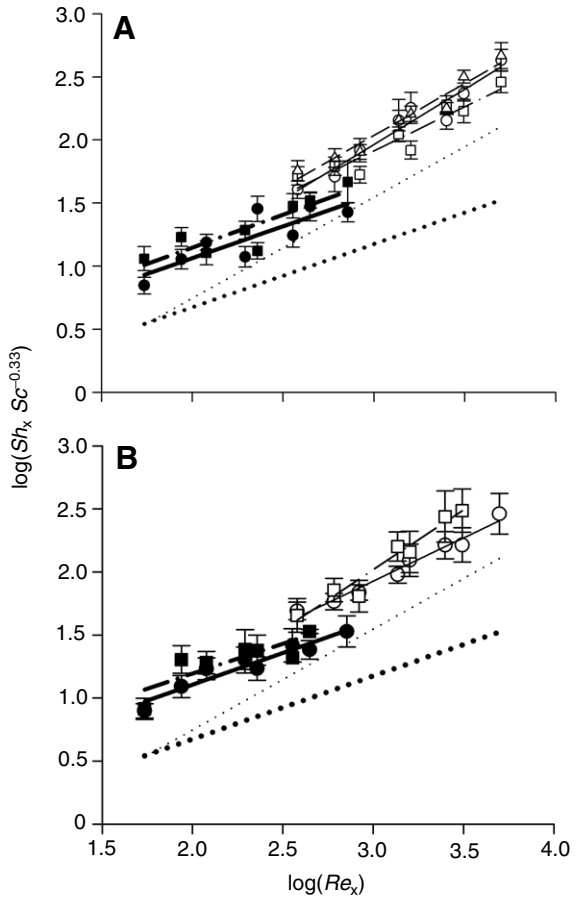

Fig. 3. The log-transformed local Sherwood number (Sh_x) and local Reynolds number (Re_x) at the upstream and downstream locations of *Vallisneria spiralis* and *Vallisneria americana* in a flat and twisted configuration at (A) 17.1 mmol m^{-3} CO_2 and (B) 1.71 mmol m^{-3} CO_2. Solid lines are model fits for *V. spiralis*, dash-dotted lines are for *V. americana* in a flat configuration, and the broken lines are for *V. americana* in a twisted configuration. The thin dotted line indicates the theoretical turbulent Sh_x, and the thick dotted line indicates the theoretical laminar Sh_x based on Eqn 9. Values are means ± s.e.m. *N* and symbols are as in Fig. 2.

and the individual regressions for each species-leaf configuration and measurement location were significant (r^2>0.68, P<0.05; see Table 2A). There were no significant differences among slopes (i.e. logB) at the upstream location (P>0.05), which was similar to previous results for *V. americana* (0.45±0.04) (Nishihara and Ackerman, 2006) and for theoretical laminar mass transport over a flat plate (0.5) (Schuepp, 1993). Whereas the intercepts were not significant, they were much greater than the theoretical value for parameter A for a constant surface flux boundary condition in a laminar boundary layer [i.e. $\log(0.464Sc^{-0.33})$=–1.18 (Schlichting and Gersten, 2000)]. In contrast, the slopes at the downstream location were heterogeneous (P<0.05; Table 2A), although a multiple comparisons test, indicated that the slopes for *V. spiralis* (0.87±0.09) and *V. americana* (0.82±0.07) in the twisted configuration at 17.1 mmol m^{-3} CO_2 were similar (P>0.05), as were *V. americana* at 17.1 mmol m^{-3} CO_2 (0.70±0.10) and *V. spiralis* at 1.71 mmol m^{-3} CO_2 (0.69±0.05). The slopes determined at the downstream location were of similar order to the theoretical value for mass transport in a turbulent concentration boundary layer over a flat plate (0.8) (Kays et al., 2005). The log-transformed intercepts (P>0.05) were not significantly different from zero; however, they were greater than predicted by a theoretical turbulent concentration boundary layer [i.e. $\log(0.030Sc^{-0.33})$=–2.37 (Schlichting and Gersten, 2000)].

The shear velocities determined from the PIV ranged from 0.040±0.002 to 0.7±0.1 cm s^{-1}, and the u^* values at the upstream locations were always greater than those measured at the downstream location at each velocity (Table 3). Moreover, u^* increased with freestream velocity for all species-leaf configurations and measurement locations. The Sh_x determined from hydrodynamic measurements (i.e. PIV results) also increased with increasing Re_x (Fig. 4). The slope of the Sh_x–Re_x regression did not vary with measurement location ($F_{(1,39)}$=0.21, P=0.65), which is in contrast to the Sh_x determined from the O_2 concentration boundary layer. However, there was a species-leaf configuration effect ($F_{(2,40)}$=4.53, P=0.017), where the slope for the regressions at the downstream location of *V. americana* in the twisted configuration was significantly different from all the other slopes (P<0.05), except for the slope determined at the downstream location of *V. spiralis* (Table 2B). The intercepts determined at the upstream locations were significantly different from zero (P<0.05), in contrast to the downstream locations (Table 2). Regardless, these values were also larger than that predicted by the turbulent concentration boundary layer.

Concentration boundary layer

The δ_{CBL} determined from the O_2 profiles and the δ_{DSL} determined from the PIV measurements decreased with increasing velocity and Re_x for both species-leaf configuration and measurement location (Fig. 5). Whereas δ_{CBL} determined from the O_2 profiles appeared similar in shape and thickness at both locations (Fig. 5A,C), the δ_{CBL} was thinner at the upstream location when normalized to distance from the leading edge of the leaf (i.e. plotted *vs* Re_x) (Fig. 5B,D). ANCOVA revealed that measurement location affected the rate of change of the thickness of the δ_{CBL} with respect to Re_x [i.e. $\log(\delta_{CBL}x^{-1}Sc^{-0.33})$ varied with Re_x] and significant differences were detected between measurement locations ($F_{(2,64)}$=8.53, P<0.0001). The slopes of the regressions at the upstream location were homogeneous (P>0.05), whereas they were heterogeneous at the downstream location (P<0.05; Table 4). The slopes of *V. spiralis* at both CO_2 concentrations were similar (P>0.05), as were both leaf configurations of *V. americana* (P>0.05) at both CO_2 concentrations (Table 4). There was some overlap between the species-leaf configurations, where the slopes *V. spiralis* at 1.71 mmol m^{-3} CO_2 were similar to those of *V. americana* and the slopes of *V. americana* at

Table 2. *Parameters of the mass transfer equation for the upstream and downstream locations of Vallisneria spiralis and Vallisneria americana (flat and twisted configurations) determined from O_2 profiles and through theoretical formulations using measurements of the velocity gradient by digital particle image velocimetry*

Measurement technique	[CO_2] (mmol m^{-3})	Species	*N*	Location	Slope	Intercept	r^2	*P*	
(A) Microsensor	17.1	*V. spiralis*	6	US	0.50±0.13	0.06±0.30	0.72	***	a
	17.1	*V. spiralis*	6	DS	0.87±0.09	–0.66±0.30	0.94	***	b
	17.1	*V. americana*	6	US	0.52±0.11	0.11±0.26	0.78	***	a
	17.1	*V. americana*	6	DS	0.70±0.10	–0.18±0.32	0.89	***	c
	17.1	*V. americana* (twisted)	8	DS	0.82±0.07	–0.43±0.22	0.96	***	b
	1.71	*V. spiralis*	9	US	0.50±0.06	0.10±0.14	0.92	***	a
	1.71	*V. spiralis*	9	DS	0.69±0.05	–0.13±0.14	0.97	***	c
	1.71	*V. americana*	6	US	0.47±0.14	0.25±0.33	0.68	*	a
	1.71	*V. americana*	6	DS	0.95±0.09	–0.83±0.29	0.95	***	–
(B) PIV	NA	*V. spiralis*	NA	US	0.68±0.08	–0.56±0.19	0.92	***	–
	NA	*V. spiralis*	NA	DS	0.70±0.06	–0.06±0.20	0.95	***	e
	NA	*V. americana*	NA	US	0.80±0.12	–0.83±0.28	0.88	***	d
	NA	*V. americana*	NA	DS	0.80±0.06	–0.34±0.19	0.97	***	–
	NA	*V. americana* (twisted)	NA	US	0.77±0.06	–0.63±0.14	0.96	***	d
	NA	*V. americana* (twisted)	NA	DS	0.66±0.08	0.05±0.25	0.94	***	e

Mass transfer equation: $Sh_x = A Re_x^B Sc^C$ (C=0.33), where A is slope and B is $10^{intercept}$, for upstream (US) and downstream (DS) locations.
PIV, digital particle image velocimetry; NA: not applicable.
Values for slope and intercept are means ± s.e.m. *P<0.05; ***P<0.001. Lowercase letters indicate slopes that are similar statistically.

Table 3. *The shear velocities at the upstream and downstream locations of Vallisneria spiralis and Vallisneria americana (flat and twisted configurations) determined using measurements of the velocity gradient of eight freestream velocities by digital particle image velocimetry*

Species (leaf configuration)	Location	Shear velocity U (cm s^{-1})							
		0.5	0.8	1.1	1.8	2.1	3.3	4.1	6.6
V. spiralis	US	0.05±0.01	0.09±0.02	0.09±0.02	0.12±0.02	0.11±0.01	0.15±0.02	0.26±0.03	0.45±0.03
V. spiralis	DS	0.10±0.01	0.18±0.01	0.16±0.01	0.23±0.04	0.23±0.01	0.42±0.01	0.46±0.01	0.66±0.02
V. americana	US	0.04±0.18	0.11±0.01	0.06±0.01	0.14±0.01	0.12±0.02	0.22±0.01	0.28±0.03	0.35±0.02
V. americana	DS	0.11±0.02	0.12±0.01	0.15±0.01	0.32±0.01	0.30±0.03	0.41±0.01	0.55±0.06	0.72±0.12
V. americana (twisted)	US	0.06±0.02	0.11±0.01	0.10±0.02	0.18±0.02	0.24±0.01	0.27±0.02	0.35±0.03	0.44±0.04
V. americana (twisted)	DS	0.10±0.02	0.15±0.02	0.21±0.04	0.22±0.02	No data	0.29±0.01	0.38±0.01	0.72±0.06

US, upstream; DS, downstream locations.

1.71 mmol m^{-3} CO_2 were similar to those of *V. spiralis*. The δ_{CBL} among species-leaf configuration, measurement location and CO_2 concentration were similar (P>0.05); however, the average δ_{CBL} values at both measurement locations were thinner at the upstream (48±2%) and downstream locations (21±1%) compared to the theoretical δ_{CBL} (based on Eqn 7).

The diffusive sublayer thickness (δ_{DSL}) determined from Eqn 8, using the measured shear velocities, was similar in thickness to theoretical estimates of the δ_{DSL} determined from the 1/7 power law (White, 1999) at the leading edge (106±6% of the theoretical δ_{DSL}; Fig. 5E) whereas at the trailing edge the δ_{DSL} was 51±2% of the theoretical δ_{DSL} (Fig. 5E,F).

Discussion

O_2 flux

The rates of physiological processes were found to vary among closely related aquatic angiosperm species and the rates were influenced by mass transport. The complexity of these interactions is evident in this study, where the effects of CO_2 concentration, freestream velocity and measurement location along a leaf surface affected the photosynthesis rates of *V. spiralis* and *V. americana* (Fig. 2). The effects of increasing CO_2 concentrations on photosynthesis are well documented, but the spatial variation is not (Invers et al., 2001; Lobban and Harrison, 1994; Schippers et al., 2004; Nielsen et al., 2006). In this study, O_2 flux was similar in both species at low CO_2

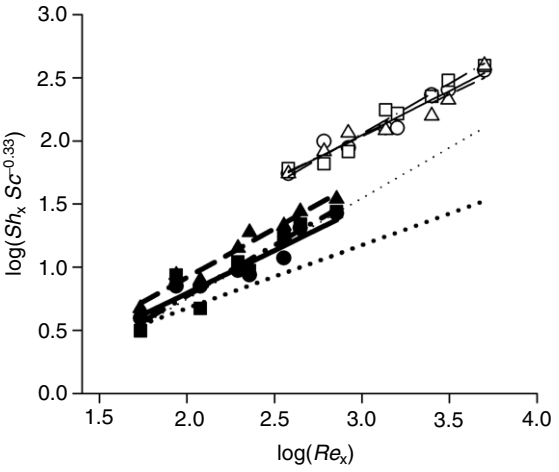

Fig. 4. The log-transformed local Sherwood number (Sh_x) and local Reynolds number (Re_x) at the upstream and downstream locations of *Vallisneria spiralis* and *Vallisneria americana* in a flat and twisted configuration determined from the mass transfer coefficient ($Sh_x=k_c x D^{-1}$; where $k_c=0.1u^*Sc^{-0.67}$) calculated using the shear velocity (u^*) measured using PIV measurements. The thin dotted line indicates the theoretical turbulent Sh_x, and the thick dotted line indicates the theoretical laminar Sh_x, based on Eqn 7, Eqn 9, and the 1/7 power-law (White, 1998). Symbols are as in Fig. 2.

concentrations. However, increasing the CO_2 concentration only enhanced the photosynthesis rates of *V. spiralis*, with no effect on *V. americana*. It is evident that *V. spiralis* is better able to respond to the higher CO_2 concentrations and increase its O_2 flux.

The difference in O_2 flux between *V. spiralis* and *V. americana* is likely due to physiological (Fig. 2A) rather than morphological differences, given that the twisted configuration of *V. americana* did not enhance O_2 flux through increases in the mass transfer coefficient (see below). Moreover, given that DIC was held constant and that the HCO_3^- concentrations at both CO_2 concentrations were similar (i.e. 460 mmol m^{-3} HCO_3^-), the increase in O_2 flux with increases in CO_2 concentration implies that the flux of CO_2 is greater for *V. spiralis* than *V. americana*. Regardless of the ability to use both CO_2 and HCO_3^- (Prins et al., 1980; Madsen and Sand-Jensen, 1991), the enhancement of O_2 flux in *V. spiralis* suggests differences in CO_2 affinity between the two species, namely that *V. spiralis* has a higher affinity for CO_2. Such variations in CO_2 affinity are not uncommon, and in general freshwater macrophytes that depend on CO_2 as the sole source of carbon have the highest affinity for CO_2 (Madsen and Sand-Jensen, 1991). Freshwater macrophytes such as *V. spiralis* and *V. americana*, which are able to use HCO_3^-, are intermediate in their affinity for CO_2, whereas marine macrophytes that exist in relatively high pH waters have the lowest CO_2 affinity (Madsen and Sand-Jensen, 1991).

As already mentioned, the effect of low CO_2 concentrations was similar between the species; however, the relationship between O_2 flux and velocity varied spatially. Specifically, O_2 flux was saturated at V_{sat} >1.8±0.9 cm s^{-1} at the upstream location, but O_2 flux continued to increase with velocity at the downstream location (Fig. 2B). This linear relationship suggests that photosynthesis is mass transfer limited at the downstream location. However, O_2 flux did not vary spatially at the high CO_2 concentration, where the O_2 flux saturated at both measurement locations for both species (Fig. 2A). Evidently, the behavior of nutrient uptake varies spatially on leaf surfaces at low nutrient concentrations. Spatial heterogeneity in mass transport has not been incorporated in current models that couple physiology and mass transport processes (e.g. Sanford and Crawford, 2000). Although, interactions of nutrient concentrations and mass transport have been observed in the nutrient uptake rates of seagrasses (Cornelisen and Thomas, 2006), marine algae (Hurd et al., 1996) and corals (Badgley et al., 2006), and in photosynthesis rates of marine macrophytes (Wheeler, 1980), periphyton (Larkum et al., 2003) and *V. americana* (Nishihara and Ackerman, 2006), little is known about how freestream velocities affect the spatial variability in nutrient uptake.

The saturating behavior of O_2 flux at the upstream location and the linearly increasing behavior of O_2 flux at the downstream location suggest that upstream uptake and associated decrease of nutrients in the concentration boundary layer impact physiological processes occurring downstream (e.g. Chambré and Acrivos, 1956; Ackerman et al., 2001). The mechanism(s) responsible for the downstream decrease in O_2 flux observed in this study has yet to be determined; however, it is likely that the surface concentrations of nutrients decrease with downstream distance from the leading edge as a result of nutrient depletion in the concentration boundary layer.

Mass transfer

The consistency of parameter B in the relationship between Sh_x and Re_x at the upstream location (0.47–0.52) demonstrates that the concentration boundary layer was laminar at that location (Fig. 3, Table 2) (Schlichting and Gersten, 2000). Conversely, parameter B differed significantly among the downstream locations (0.69 to 0.95; Fig. 3, Table 2), but none of these values were significantly different (P>0.05) from the theoretical value of mass transport in a turbulent concentration boundary layer (B=0.8) (Schlichting and Gersten, 2000). Based on these observations and those of an earlier study (Nishihara and Ackerman, 2006), it is apparent that the concentration boundary layer of *V. spiralis* and *V. americana* shifts from a laminar to turbulent regime between Re_x of 700 to 1500. These values are considerably lower than the transitional velocity for momentum over a smooth flat plate ($Re_x=3\times10^5$) (Schlichting and Gersten, 2000), but are similar to mass transport phenomena in terrestrial plant leaves in a turbulent freestream (e.g. Re_x=1860) (Schuepp, 1993).

Given that surface corrugations on a flat surface were demonstrated to increase mass transfer rates in engineering applications (Tzanetakis et al., 2004), the twisted morphology of *V. spiralis* was predicted to enhance mass transport. However, the similar shape obtained by twisting *V. americana*

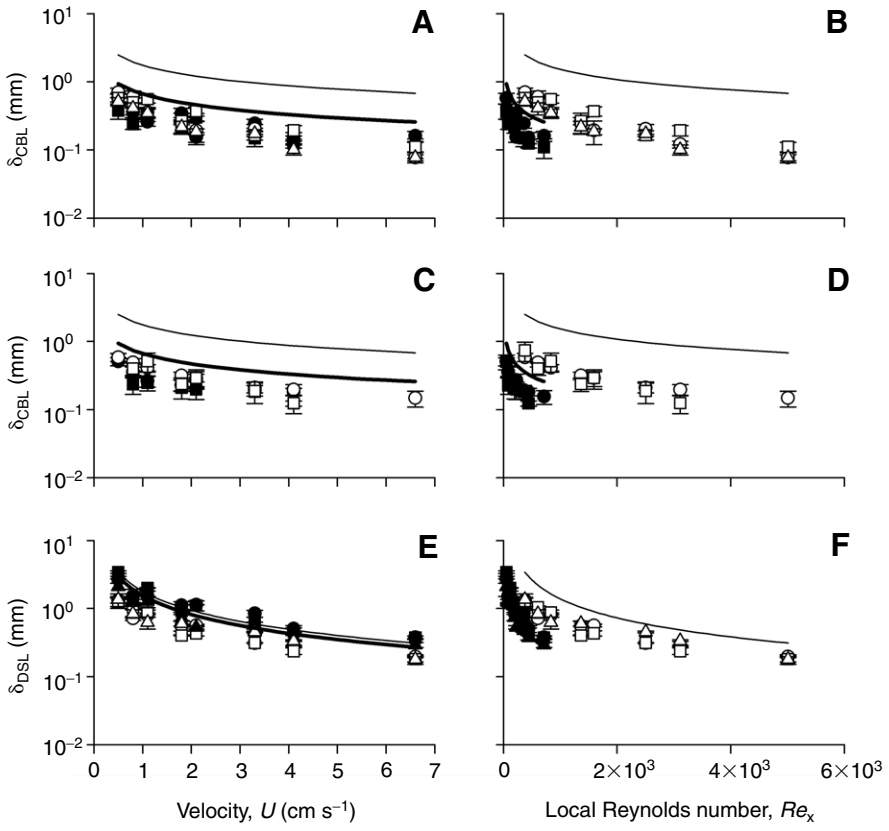

Fig. 5. The concentration boundary layer (CBL) thickness (δ_{CBL}) at the upstream and downstream locations of *Vallisneria spiralis* and *Vallisneria americana* in a flat and twisted configuration. (A) and (B) are the δ_{CBL} *vs* the freestream velocity (U) and the local Reynolds number (Re_x), respectively, at 17.1 mmol m^{-3} CO_2. (C,D) The δ_{CBL} *vs* the U and Re_x, respectively, at 1.71 mmol m^{-3} CO_2; (E,F) diffusive sublayer thickness (δ_{DSL}) determined from hydrodynamic measurements *vs* U and Re_x, respectively. The thick and thin solid lines indicate the theoretical δ_{CBL} (A–D) and the theoretical δ_{DSL} at the upstream and downstream locations (E,F), respectively.

did not enhance mass transfer rates (Fig. 3A,B). This is consistent with the observation that undulations in the blades of the marine macrophyte *Macrocystis integrifolia* did not to enhance inorganic nitrogen uptake (Hurd et al., 1996). However, the assimilation of DIC has been recently reported to be related to plant architecture in aquatic angiosperms (Nielsen et al., 2006) and similar morphological effects on nutrient uptake have been reported in corals (Lesser et al., 1994; Helmuth et al., 1997). It is possible that the effect of the twist in *V. americana* was not detected, due to limitations in the microsensor technique (see below). Clearly, the influence of morphological features in mass transport remains an equivocal issue (cf. Thomas and Atkinson, 1997).

Concentration boundary layer

Concentration boundary layers can be estimated through direct measurements of the scalar (e.g. O_2) profile, or indirectly by measuring the hydrodynamic boundary layer and multiplying by a scaling factor (e.g. $Sc^{-0.33}$) (Dade, 1993). It is common to describe the thickness of the concentration boundary layer that forms around the surface of macrophytes and refer to it as 'boundary layer resistance' to mass transport (Wheeler, 1980; Stevens and Hurd, 1997; Larkum et al., 2003). In this case, the δ_{CBL} is given by $\delta_{CBL}=J/(C_S-C_B)$, by assuming that the surface concentration is zero (i.e. the surface is a perfect sink) (Wheeler, 1980; Stevens and Hurd, 1997; Larkum et al., 2003). However, the δ_{CBL} determined by this method, may overestimate δ_{CBL} (Stevens and Hurd, 1997; Larkum et al., 2003) as previously demonstrated (Nishihara and Ackerman, 2006), where the δ_{CBL} values determined from O_2 profiles were >63% smaller than the δ_{CBL} values determined by using the boundary layer resistance model. These observations suggest that the two assumptions (i.e. spatially homogeneous flux and a perfect sink condition) invoked to determine the δ_{CBL} values may be inappropriate. For example, saturating nutrient uptake rates at high velocities indicate kinetic limitation (i.e. mass transfer rates > nutrient uptake rates), which would occur if the nutrient is in excess and the surface concentration is >0 (Nishihara and Ackerman, 2006). It is apparent that indirect estimates of the concentration boundary layer from hydrodynamic theory overestimate mass transfer rates in aquatic macrophytes.

The importance of direct measurements of the concentration boundary layer led to the application of O_2 microsensors in boundary layer research, such as those used in this and other studies (Glud et al., 1994; Larkum et al., 2003; Nishihara and Ackerman, 2006; Nishihara and Ackerman, 2007). Evidence suggests that microsensors directly affect the concentration boundary layer and revealed that the concentration boundary layer, determined by the δ_{DSL}, was reduced to 55–75% of the theoretical δ_{DSL} (Glud et al., 1994). It is difficult to assess whether the decrease in the concentration boundary thickness was caused by the microsensor, given that the hydrodynamic boundary layer was not characterized in that study (Glud et al., 1994). However, it has been suggested that the microsensor has little impact on the concentration boundary layer at low Reynolds number (Re_d) of the microsensor [~6 (Hondzo et al., 2005)], which ranged from 0.14 to 1.8 in this study. Therefore, near the surface of the leaf, where velocities are lower than the freestream velocity (i.e. viscous flow, Re_d <1), the flow remains attached to the microsensor. Nevertheless, δ_{CBL} measured with the microsensors were ⩽48% of the theoretical δ_{CBL} at the upstream location, which is less that what is predicted by microsensor-induced compression (Glud et al., 1994).

Table 4. *The slope and intercept of regressions*† *for the upstream and downstream locations of Vallisneria spiralis and Vallisneria americana (flat and twisted configuration) determined directly from O_2 profiles*

$[CO_2]$ (mmol m^{-3})	Species	*N*	Location	Slope	Intercept	r^2	*P*	
17.1	*V. spiralis*	6	US	–0.47±0.12	0.31±0.29	0.67	**	a
17.1	*V. spiralis*	6	DS	–0.82±0.09	0.93±0.27	0.93	***	b
17.1	*V. americana*	6	US	–0.51±0.11	0.30±0.26	0.74	**	a
17.1	*V. americana*	6	DS	–0.68±0.10	0.55±0.31	0.87	***	c
17.1	*V. americana* (twisted)	8	DS	–0.74±0.07	0.64±0.21	0.95	***	c
1.71	*V. spiralis*	9	US	–0.46±0.06	0.24±0.14	0.89	***	a
1.71	*V. spiralis*	9	DS	–0.63±0.04	0.39±0.12	0.98	***	b,c
1.71	*V. americana*	6	US	–0.44±0.12	0.15±0.27	0.67	*	a

Measurement technique = microsensor. US, upstream; DS, downstream locations.
†$\log(\delta_{CBL}x^{-1})$ *vs* $\log(Sc^{-C}Re_x)$ (C=0.33).
Values for slope and intercept are means ± s.e.m. *P<0.05; ***P<0.001. Lowercase letters indicate slopes that are statistically similar.

Therefore, the thinner δ_{CBL} may also result from the influence of biological and chemical processes on O_2 flux and concentration boundary layer thickness (Nishihara and Ackerman, 2006). Given the difficulties in measuring the O_2 profiles at high velocities (i.e. >3.3 cm s^{-1} in this study) and the possible compression effect of the microsensor, the technique used in this study may be too coarse to resolve differences between the flat and twisted leaf morphologies at moderate to high velocities.

Ecological implications

The interaction between physiology and mass transport among species is complex, and elucidating the mechanisms underlying these processes should provide insight on how environmental factors influence the biology of aquatic organisms. In addition, the diversity in these interactions makes it difficult to predict how environmental alterations including climate change will affect aquatic ecosystems. Presently, global CO_2 levels are increasing, leading to the acidification of freshwater and marine ecosystems (Harley et al., 2006). Macrophytes that are physiologically limited by present CO_2 levels may see a dramatic increase in productivity (Schippers et al., 2004). However, in marine systems, where the majority of macrophytes have low CO_2 affinity (Madsen and Sand-Jensen, 1991), the effects are likely to be small except in the limited number of marine angiosperms (i.e. seagrasses) (Invers et al., 2001). Furthermore, coupled with increased advective transport, the increase in CO_2 mass transfer rates could provide a mechanism for macrophytes with high CO_2 affinity to displace species (e.g. *V. americana*) that are less sensitive to increases in CO_2. In areas where water velocities promote high mass transfer rates, small increases in CO_2 could have a significant impact on the distribution of aquatic macrophytes. However, in marine systems, where the majority of macrophytes have low CO_2 affinity (Madsen and Sand-Jensen, 1991), the effects are likely to be small. Clearly, further research is required to elucidate the effects of mass transport on ecophysiological processes.

Conclusion

Physiological and mass transport mechanisms are coupled and in biological systems such as aquatic macrophytes these processes vary spatially. The O_2 flux was higher in *V. spiralis* than in *V. americana* when CO_2 concentrations were high, but were similar at the lower CO_2 concentration. Importantly, the O_2 flux varied spatially on the leaf surface at low CO_2 concentrations, where O_2 flux (i.e. photosynthesis) was kinetically limited at the upstream location and mass transfer limited at the downstream location. Further studies are needed to elucidate the effects of morphology on mass transport and the mechanisms underlying the spatial heterogeneity of O_2 flux and mass transfer rates. Mass transport relationships must be considered to properly evaluate how changes in environmental conditions affect the productivity of aquatic ecosystems.

List of abbreviations and symbols

δ_{CBL}	concentration boundary layer thickness (m)
δ_{DSL}	diffusive sublayer thickness (m)
ΔC	concentration gradient (mmol m^{-3})
θ	dimensionless concentration
κ	von Karman constant
ν	molecular diffusivity of momentum (m^2 s^{-1})
ρ	density of water (kg m^{-3})
τ	boundary shear stress (Pa)
a,b	constants to Eqn 1 (m^{-1})
A,B,C	constants to Eqn 6
C	nutrient concentration (mmol m^{-3})
C_S	surface concentration (mmol m^{-3})
C_B	bulk water concentration (mmol m^{-3})
CBL	concentration boundary layer
chl_{a+b}	total chlorophyll a + b concentration
DSL	diffusive sublayer
D	molecular diffusivity (m^2 s^{-1})
DIC	dissolved inorganic carbon
J	O_2 flux (mmol m^{-2} s^{-1})
J_{max}	maximum O_2 flux (mmol m^{-2} s^{-1})

J_{chla+b}	Chlorophyll a+b normalized O_2 flux [mmol m^{-2} s^{-1} (g_{chla+b} m^{-2})$^{-1}$]
k_c	mass transfer coefficient (m s^{-1})
PAR	photosynthetically active radiation (μmol photon m^{-2} s^{-1})
P_{max}	maximum oxygen flux [mmol m^{-2} s^{-1} (g_{chla+b} m^{-2})$^{-1}$]
PIV	particle image velocimetry
Re_d	microsensor Reynolds number
Re_x	local Reynolds number
Sc	Schmidt number
Sh_x	local Sherwood number
u^*	shear velocity (m s^{-1})
U	freestream velocity (m s^{-1})
V	half-saturation velocity (m s^{-1})
V_{sat}	saturation velocity (m s^{-1})
x	distance from the leading edge of the leaf (m)
z	height above leaf surface (m)

The authors would like to thank Patrick Ragaz for assistance with the PIV. This research was supported in part by funding from the University of Guelph and the Natural Sciences and Engineering Research Council of Canada to J.D.A.

References

Ackerman, J. D. and Hoover, T. M. (2001). Measurement of local bed shear stress in streams using a Preston-static tube. *Limnol. Oceanogr.* **46**, 2080-2087.

Ackerman, J. D., Loewen, M. R. and Hamblin, P. F. (2001). Benthic-pelagic coupling over a zebra mussel reef in western Lake Erie. *Limnol. Oceanogr.* **46**, 892-904.

Badgley, B. D., Lipschultz, F. and Sebens, K. P. (2006). Nitrate uptake by the reef coral *Diploria stribosa*: effects of concentration, water flow, and irradiance. *Mar. Biol.* **149**, 327-338.

Chambré, P. L. and Acrivos, A. (1956). On chemical surface reactions in laminar boundary layer flows. *J. Appl. Phys.* **27**, 1322-1328.

Cornelisen, C. D. and Thomas, F. M. (2006). Water flow enhances ammonium and nitrate uptake in a seagrass community. *Mar. Ecol. Prog. Ser.* **312**, 1-13.

Dade, W. B. (1993). Near-bed turbulence and hydrodynamic control of diffusional mass transfer at the sea floor. *Limnol. Oceanogr.* **38**, 52-69.

Falter, J. L., Atkinson, M. J. and Coimbra, C. F. M. (2005). Effects of surface roughness and oscillatory flow on the dissolution of plaster forms: evidence for nutrient mass transfer to coral reef communities. *Limnol. Oceanogr.* **50**, 246-254.

Glud, R. N., Gundersen, J. K., Revsbech, N. P. and Jørgensen, B. (1994). Effects on the benthic boundary layer imposed by microelectrodes. *Limnol. Oceanogr.* **39**, 462-467.

Harley, C. D. G., Hughes, A. R., Hultgren, K. M., Miner, B. G., Sorte, C. J. B., Rodriguez, L. F., Tomanek, L. and Williams, S. L. (2006). The impacts of climate change in coastal marine systems. *Ecol. Lett.* **9**, 228-241.

Helmuth, B. S. T., Sebens, K. P. and Daniel, T. L. (1997). Morphological variation in coral aggregations: branch spacing and mass flux to coral tissues. *J. Exp. Mar. Biol. Ecol.* **209**, 233-259.

Hondzo, M., Feyaerts, T., Donovan, R. and O'Conner, B. L. (2005). Universal scaling of dissolved oxygen distribution at the sediment–water interface: a power-law. *Limnol. Oceanogr.* **50**, 1667-1676.

Hurd, C. L., Harrison, P. J. and Druehl, L. D. (1996). Effect of seawater velocity on inorganic nitrogen uptake by morphologically distinct forms of *Macrocystis integrifolia* from wave-sheltered and exposed sites. *Mar. Biol.* **126**, 205-214.

Invers, O., Zimmerman, R. C., Alberte, R. S., Perez, M. and Romero, J. (2001). Inorganic carbon sources for seagrass photosynthesis: an experimental evaluation of bicarbonate use in species inhabiting temperate waters. *J. Exp. Mar. Biol. Ecol.* **265**, 203-271.

Jana, S. and Choudhuri, M. A. (1980). Senescence in submerged aquatic angiosperms: changes in intact and isolated leaves during aging. *New Phytol.* **86**, 191-198.

Kays, W. M., Crawford, M. E. and Weigand, B. (2005). *Convective Heat and Mass Transfer* (4th edn). New York: McGraw-Hill.

Larkum, A. W. D., Koch, E. M. and Kuhl, M. (2003). Diffusive boundary layers and photosynthesis of the epilithic algal community of coral reefs. *Mar. Biol.* **142**, 1073-1082.

Lesser, M. P., Weis, V. M., Patterson, M. R. and Jokiel, P. L. (1994). Effects of morphology and water motion on carbon delivery and productivity in the reef coral, *Pocillopora damicornis* (Linnaeus): diffusion barriers, inorganic carbon limitation, and biochemical plasticity. *J. Exp. Mar. Biol. Ecol.* **178**, 153-179.

Lobban, C. S. and Harrison, P. J. (1994). *Seaweed Ecology and Physiology.* New York: Cambridge University Press.

Maberly, S. C. and Madsen, T. V. (1998). Affinity for CO_2 in relation to the ability of freshwater macrophytes to use HCO_3^-. *Funct. Ecol.* **12**, 99-106.

Madsen, T. M. and Sand-Jensen, K. (1991). Photosynthetic carbon assimilation in aquatic macrophytes. *Aquat. Bot.* **41**, 5-40.

Nielsen, H. D., Nielsen, S. L. and Madsen, T. V. (2006). CO_2 uptake patterns depend on water current velocity and shoot morphology in submerged stream macrophytes. *Freshw. Biol.* **51**, 1331-1340.

Nishihara, G. N. and Ackerman, J. D. (2006). The effect of hydrodynamics on the mass transfer of dissolved inorganic carbon to the freshwater macrophyte *Vallisneria americana*. *Limnol. Oceanogr.* **51**, 2734-2745.

Nishihara, G. N. and Ackerman, J. D. (2007). On the determination of mass transfer in a concentration boundary layer. *Limnol. Oceanogr. Methods* In Press.

Nishihara, G. N., Terada, R. and Noro, T. (2005). Effect of temperature and irradiance on the uptake of ammonium and nitrate by *Laurencia brongniartii* (Rhodophyta, Ceramiales). *J. Appl. Phycol.* **17**, 371-377.

Phillips, J. C. and Hurd, C. L. (2004). Kinetics of nitrate, ammonium, and urea uptake by four intertidal seaweeds from New Zealand. *J. Phycol.* **40**, 534-545.

Pip, E. (1984). Ecogeographical tolerance range variation in aquatic macrophytes. *Hydrobiologia* **108**, 37-48.

Prins, H. B. A., Snel, J. F. H., Helder, R. J. and Zanstra, P. E. (1980). Photosynthetic HCO_3^- utilization and OH^- excretion in aquatic angiosperms. *Plant Physiol.* **66**, 818-822.

Sanford, L. P. and Crawford, S. M. (2000). Mass transfer versus kinetic control of uptake across solid-water boundaries. *Limnol. Oceanogr.* **45**, 1180-1186.

Schippers, P., Vermaat, J. E., de Klein, J. and Mooij, W. M. (2004). The effect of atmospheric carbon dioxide elevation on plant growth in freshwater ecosystems. *Ecosystems* **7**, 63-74.

Schlichting, H. and Gersten, K. (2000). *Boundary Layer Theory* (8th edn). Berlin: Springer-Verlag.

Schuepp, P. H. (1993). Leaf boundary layers. *New Phytol.* **125**, 477-507.

Sculthorpe, C. D. (1967). *The Biology of Aquatic Vascular Plants.* London: Edward Arnold.

Stevens, C. L. and Hurd, C. L. (1997). Boundary-layers around bladed aquatic macrophytes. *Hydrobiologia* **346**, 119-128.

Stumm, W. and Morgan, J. J. (1996). *Aquatic chemistry* (3rd edn). New York: John Wiley.

Thomas, F. I. M. and Atkinson, M. J. (1997). Ammonium uptake by coral reefs: effects of water velocity and surface roughness on mass transfer. *Limnol. Oceanogr.* **42**, 81-88.

Tzanetakis, N., Scott, K., Taama, W. M. and Jachuck, R. J. J. (2004). Mass transfer characteristics of corrugated surfaces. *Appl. Therm. Eng.* **24**, 1865-1875.

Wheeler, W. M. (1980). Effect of boundary layer transport on the fixation of carbon by the giant kelp, *Macrocystis pyrifera*. *Mar. Biol.* **56**, 103-110.

White, F. M. (1999). *Fluid Mechanic* (4th edn). New York: WCB McGraw-Hill.